PHYSICAL REVIEW B VOLUME 23, NUMBER 12 15 JUNE 1981

Electrical and thermal transport coefficients of pure vanadium

C. L. Tsai,* R. L. Fagaly,† and H. Weinstock
Department of Physics, Illinois Institute of Technology, Chicago, Illinois 60616

F. A. Schmidt
Ames Laboratory, Department of Energy, Ames, Iowa 50011

(Received 10 March 1980)

The electrical and thermal conductivities of high-purity vanadium samples have been measured over a wide range of low temperatures and analyzed in terms of electron-impurity scattering, electron-electron scattering, and electron-phonon interband and intraband scattering. In the normal state, electron-phonon interband scattering is a major factor over the entire temperature range, with the electron-phonon intraband scattering becoming important above 50 K. At lower temperatures, our results show evidence of electron-electron scattering. The thermal conductivity in the superconducting state was fit by Bardeen-Rickayzen-Tewordt theory, with $2\Delta(0)/k_B T_c \simeq 3.386$. The deviation of the experimental points from this fit at lower temperatures was used to obtain the lattice conductivity, providing additional information on the phonon-electron interaction and phonon-boundary scattering. The mass-enhancement factor, λ, is also calculated and found to be consistent with those values obtained from specific-heat and tunneling-effect measurements.

I. INTRODUCTION

It is well documented that the electron-electron interaction is an important scattering mechanism in transition metals.[1] However, there has been no reported evidence of this mechanism in vanadium except for a preliminary report of the current work.[2] Although the electron-electron interaction appears to be small, it is observable at lower temperatures in high-purity vanadium.

There were a number of previous investigations of vanadium,[3] the latest being carried out by Jung *et al.*[4] on several pure specimens. We have extended their electrical and thermal-conductivity measurements to below the superconducting transition temperature T_c on high-purity samples in order to obtain more information on the scattering mechanisms of electrons and phonons. Our primary aim was to search for evidence of an electron-electron interaction, in addition to electron-impurity scattering, and electron-phonon interband and intraband scattering. The scattering mechanisms for phonons, such as phonon-boundary scattering, phonon-impurity scattering, and phonon-electron scattering also will be discussed.

Our experimental details and results are presented in Sec. II. The analysis of the experimental data and the discussion are in Sec. III, and our conclusions are presented in Sec. IV.

II. EXPERIMENTAL DETAILS AND RESULTS

A. Apparatus

Both the thermal-conductivity and electrical-resistivity measurements were made in a He cryostat described earlier.[5] The thermal conductivity was measured using a potentiometric method.[1,6] This method differs from the conventional two thermometers-one heater method[7] in that ΔT is not determined by subtracting the temperatures (derived from the resistances) of the two thermometers. Instead, ΔT is found from the differential in resistance (ΔR) between the two thermometers with the power on, i.e.,

$$\Delta T = -\left(\frac{\partial T}{\partial R}\right)\Delta R - \frac{1}{2}\left(\frac{\partial^2 T}{\partial R^2}\right)(\Delta R)^2 . \quad (1)$$

This method is particularly insensitive to drifts in the base temperature. Another advantage of this method is that only one thermometer calibration need be used, implying uncertainty in only one thermometer calibration rather than in two. In order to cover the temperature range from 0.4 to 30 K, each thermode consisted of three different Allen-Bradley carbon resistors. In addition, the corresponding carbon resistors at the two thermodes were carefully chosen to have matching resistance-versus-temperature characteristics [and, with hope, identical $(\partial R/\partial T)$'s]. The details of this potentiometric method are discussed elsewhere.[6,8] A three-wire ac bridge was used to measure the resistance of each thermometer, as well as the resistance difference of the corresponding pair of carbon thermometers. Each carbon resistor was calibrated against a germanium resistance thermometer[9] in the range 0.4–2 K and against a carbon-glass resistance thermometer[10] from 2 to 30 K. A precision of better than 0.1% was achieved by fitting the resistance $R(T)$ of the various carbon resistors to the modified Clement-Quinell formula described by Kes *et al.*,[11] where

$$\left(\frac{\ln R}{T}\right)^{\alpha_t} = A + B(\ln R) + C(\ln R)^2 , \qquad (2)$$

where $\alpha_t = 0.552$ or 1.049, i.e., either gives an equally good fit.

The 0.1% uncertainty in T gives rise to an uncertainty $[\delta(\Delta T)]$ of less than 1% in ΔT, i.e., $\delta(\Delta T)/\Delta T \leq 0.01$. An SHE model 120 resistance bridge[12] was used in conjunction with an SHE model automatic temperature controller (ATC),[12] and additional carbon resistance thermometers. This produced temperature regulation to better than 1 mK at all temperatures. Heater power was determined by a four-wire dc method. The major uncertainty in both the thermal conductivity and electrical resistivity was due to the uncertainty in the geometrical factor (F) which is the ratio of the cross-sectional area (A) to the sample length (l), i.e., $F = A/l$. The uncertainty in F is less than 1.5% and gives rise to a systematic error that merely shifts the scale of either measurement and is temperature independent.

For measuring electrical resistivity (ρ), a conventional four-probe ac technique was used.[13] The rms current densities used varied between 3 and 100 A/cm^2. The largest contribution to the uncertainty in ρ (as stated above) was due to the geometric factor, which is temperature independent.

The vanadium samples were purified by one of the authors (F.A.S.) using the electrotransport technique. The details of the sample preparation and impurity concentration are discussed by Carlson *et al.*[14] Both samples had a polished surface, and resistivity measurements were made on the samples as received. The thermal conductivity of the purer sample (designated as Sample I) also was measured as received. The thermal conductivity of the less-pure sample (designated as Sample II) was first measured as received, and then remeasured after sandblasting the surfaces with 27 μm Al_2O_3 particles. This surface roughening was done to attain the (phonon-) boundary scattering regime in the low-temperature range of the superconducting-state measurements.[15]

Since the vanadium samples become superconducting below a transition temperature T_c, a superconducting magnet was used to drive the samples into the normal state when measurements in that state were desired. The applied magnetic field generally was set just higher than $H_{c2}(T)$.[16] Details of the superconducting magnet and cryostat have been described elsewhere.[8] The electrical magnetoresistance was checked at a variety of temperatures to confirm that the effect of magnetoresistance in both electrical and thermal-conductivity measurements was very small over the temperature range studied (since $\omega_c\tau < 1$).

B. Results

Figure 1 shows the electrical resistivity of the two vanadium samples. Sample I, with higher purity, had a residual resistivity of $1.09 \times 10^{-8}\Omega$ cm, and RRR ~ 1760, and a superconducting transition temperature $T_c = 5.43 \pm 0.02$ K. Sample II, with lower purity, had a residual resistivity of 2.61×10^{-7} Ω cm and a T_c of about 5.37 K.

Our electrical-resistivity measurements on both samples matched each other above 70 K where the electron-impurity scattering frequency is much less than the intrinsic electron scattering frequency. In general, our measurements in this higher-temperature range are in agreement with those of Jung *et al.*[4] Our T_c for these two samples match values obtained from specific-heat data.[17]

Figure 2 exhibits the thermal conductivity versus temperature of these two samples. Sample I had a thermal-conductivity maximum of 11.2 W/(cm K) at 8.0 K, while Sample II had a maximum of only 1.5 W/(cm K) occurring at a higher temperature, 20 K. Below T_c, the thermal conductivity in the superconducting state K_s of both samples is less than that of the normal state K_n. The fact that K_s decreases exponentially as $T \to 0$ indicates that electrons are the dominant heat carriers in the

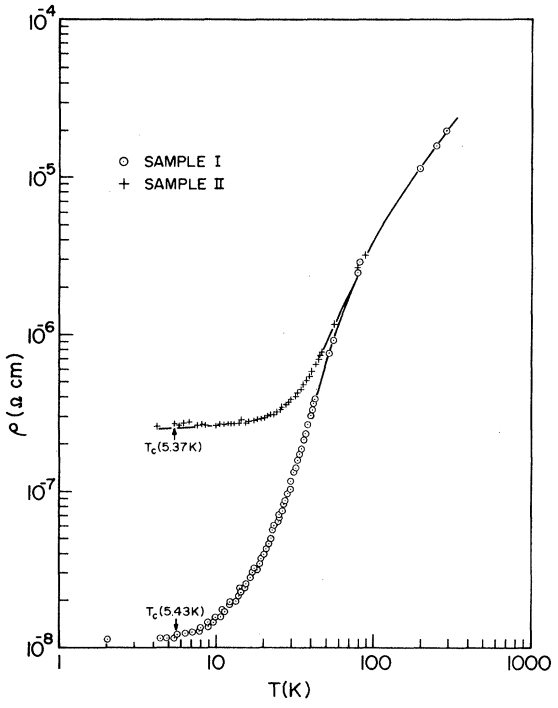

FIG. 1. Measured electrical resistivity versus temperature for two vanadium samples. The higher-purity sample (I) has an RRR ~ 1760 and $T_c = 5.43$ K; the less-pure sample (II) has $T_c = 5.37$ K.

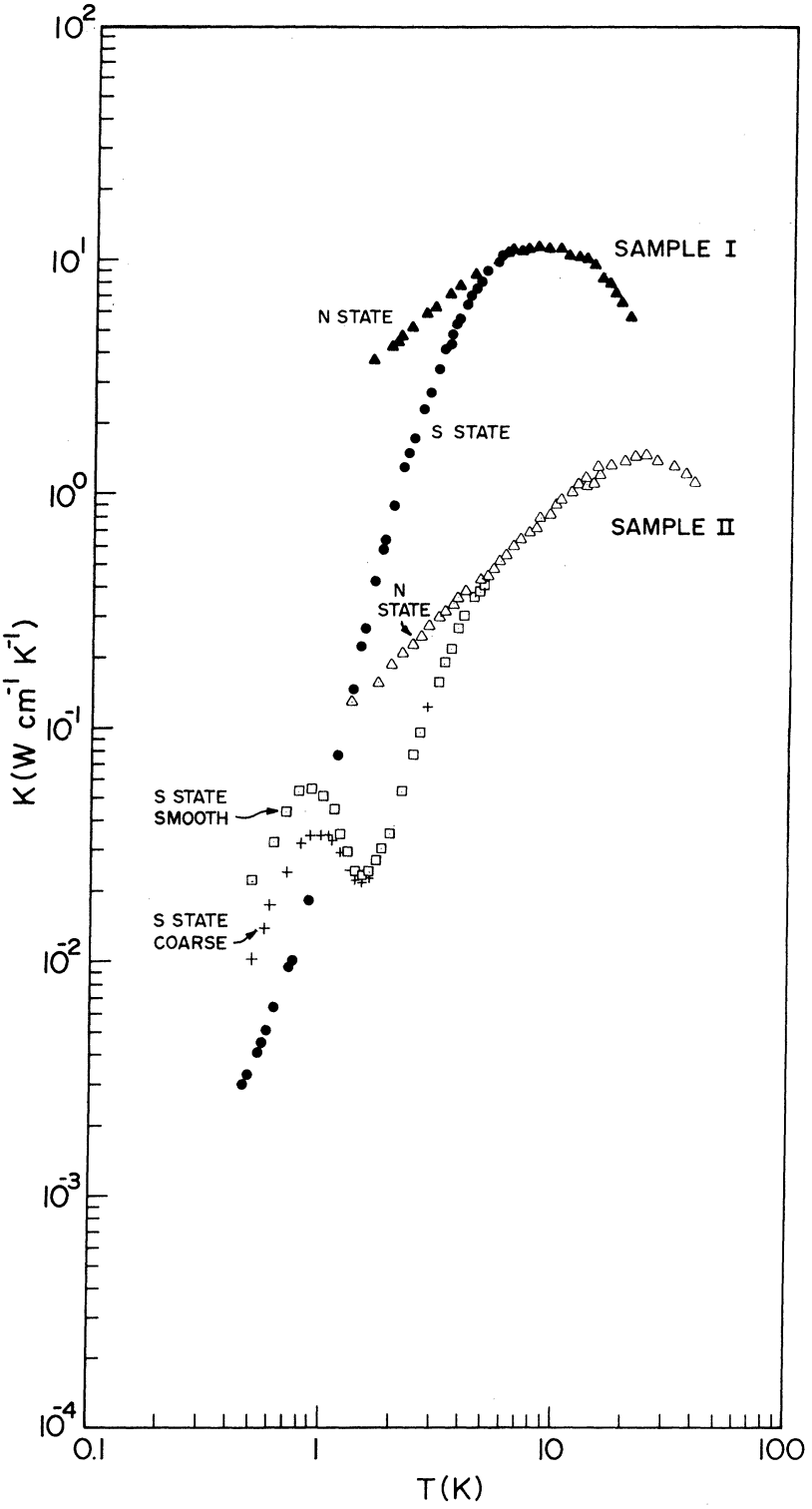

FIG. 2. Measured thermal conductivity versus temperature for both samples in the superconducting and normal states. Sample-II data were taken as received (smooth surface) and after sandblasting (rough surface). A difference occurs only for those data in the superconducting state.

normal state at low temperature. However, below 1.6 K, K_s deviates from an exponential dependence and varies as T^3 below 1.0 K. This is caused by the domination of lattice conductivity K_{gs}. It is worth noting that K_s for the two surface preparations (polished and subsequently sandblasted) of Sample II differs by a factor 2.5 at the lowest temperatures. This provides further evidence that lattice conductivity K_{gs} dominates electron conductivity K_{es} for temperatures well below T_c. In addition, K_n for Sample II was identical for both surface preparations over the entire temperature range of measurement.

Our thermal-conductivity measurements also are consistent with those of Jung *et al.*[4] in the range of temperature overlap. However, we limit our analysis to measurements below 20 K in determining contributions to the thermal resistivity from various electron scattering mechanisms.

III. ANALYSIS AND DISCUSSION

A. Analysis of electrical and thermal conductivities in the normal state

In this section the measured electrical and thermal resistivities are analyzed in terms of a variety of electron scattering mechanisms. These important mechanisms, namely electron-impurity, electron-electron, electron-phonon intraband and interband scattering, and their contributions to the electrical and thermal resistivities have been discussed in the literature.[18-24] Further, the measured resistivities were fitted in terms of a single conduction-band model, primarily because the d electrons (which we ignore) are in narrow bands and have low Fermi velocity.

Thus, assuming Matthiessen's rule to be valid,[25] the total electrical resistivity ρ can be written as

$$\rho=\rho_0+\rho_{ee}T^2+\rho_{sd}T^3\frac{J_3(\Theta_D/T)}{7.212}+\rho_{ss}T^5\frac{J_5(\Theta_D/T)}{124.42}, \tag{3}$$

where

$$J_n(\Theta_D/T)=\int_0^{\Theta_D/T}\frac{x^n e^x}{(e^x-1)^2}\,dx$$

is the nth-order Debye integral.

The first term on the right-hand side of Eq. (3) is due to electron-impurity scattering. The second term, $\rho_{ee}T^2$, is from the electron-electron (Coulomb) interaction and is observed for several transition metals. The third term is particularly important for transition metals because high-Fermi-velocity s-band electrons may be scattered into low-Fermi-velocity d-band states which act as electron traps. Last is the Bloch-Grüneisen term arising from intraband phonon scattering of electrons. In the low-temperature limit, Eq. (3) reduces to

$$\rho=\rho_0+\rho_{ee}T^2+\rho_{sd}T^3+\rho_{ss}T^5. \tag{4}$$

Thus ρ_0, ρ_{ee}, ρ_{sd}, and ρ_{ss} are the parameters used for fitting the electrical-resistivity measurements.

For thermal resistivity, both electron-phonon intraband and interband scattering give rise to a quadratic temperature dependence in the low-temperature limit.[23,24] Electron-electron scattering yields a linear term.[24] Thus, the thermal resistivity in the low-temperature limit can be written as

$$W=\frac{1}{K}=\frac{\beta_0}{T}+\beta_{ee}T+(\beta_{sd}+\beta_{ss})T^2, \tag{5}$$

$$WT=\beta_0+\beta_{ee}T^2+(\beta_{ep})T^3,$$

with

$$\beta_{ep}=\beta_{sd}+\beta_{ss},$$

where β_0, β_{ee}, and β_{ep} are the fitting parameters for thermal resistivity, with β_{sd} and β_{ss} obtainable by applying the Wiedemann-Franz law in conjunction with electrical resistivity measurements.

The scheme of our fit for electrical resistivity is as follows: In the low-temperature limit, or $T \lesssim 10$ K, we obtain an upper limit for ρ_0, ρ_{ee}, and

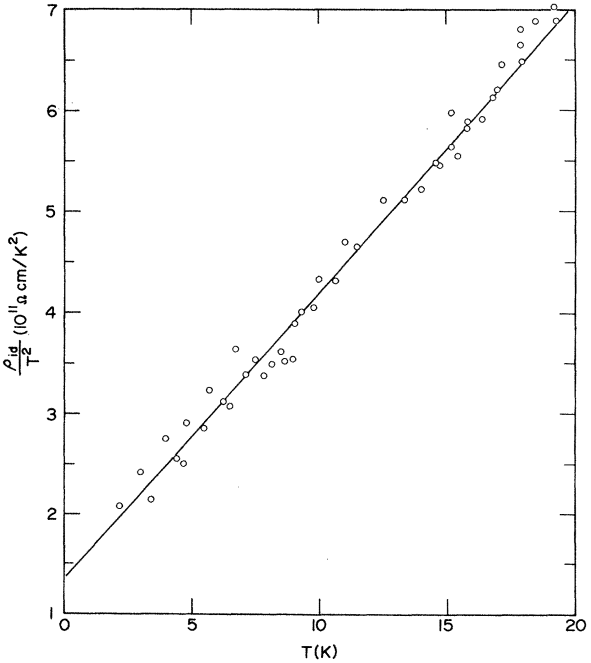

FIG. 3. Experimental data and least-squares fit of (ρ_{id}/T^2) versus T for Sample I.

TABLE I. Parameters for electrical and thermal resistivity.

Sample	ρ_0 (Ω cm)	ρ_{ee} (Ω cm/K^2)	ρ_{sd} (Ω cm/K^3)	ρ_{ss} (Ω cm/K^5)
I	1.09×10^{-8}	1.30×10^{-11}	2.75×10^{-12}	9.5×10^{-16}
II	2.62×10^{-7}		4.35×10^{-12}	
J2[a]	1.24×10^{-8}		2.74×10^{-12}	1.7×10^{-15}
J4[a]	2.3×10^{-7}		3.8×10^{-12}	

Sample	β_0(cm K^2/W)	β_{ee}(cm/W)	β_{ep}(cm/W K)
I	0.446	1.30×10^{-3}	3.09×10^{-4}
II	10.22		3.1×10^{-4}
*J2**	0.50		3.73×10^{-4}
*J4**	10		5.18×10^{-4}

[a] Taken from Jung *et al.* (Ref. 4).

ρ_{sd} by a least-squares fit of $\rho=\rho_0+\rho_{ee}T^2+\rho_{sd}T^3$. This fit is shown in Fig. 3 as $(\rho-\rho_0)/T^2$ or $(\rho_{ee}+\rho_{sd}T)$ vs T for Sample I. Then using the values obtained for the parameters ρ_0, ρ_{ee}, and ρ_{sd}, we adjusted Θ_D and then fit ρ over the entire temperature range up to 300 K. The parameters for the best fit to our electrical resistivity are listed in Table I along with those parameters for the thermal resistivity. Note that the electron-impurity scattering of Sample II is so large that it is difficult to study the electron-electron scattering in this sample. Reassuringly, the values ρ_{sd} and ρ_{ss} of Sample II did match as expected with those of Sample I. The individual contributions to the electrical resistivity of Sample I are shown in Fig. 4. It is clear that above 50 K, both *s-d* and *s-s* scattering contribute about equally to the electrical resistivity. However, the contribution of *s-s* scattering decreases dramatically below 50 K, while the *s-d* scattering still makes a substantial contribution to the resistivity. Below 10 K, the electron-electron scattering plays an important role in the electrical resistivity, since the *s-d* scattering begins to "freeze out."

It is worth noting that the ρ_{sd} values obtained are comparable with those of Jung *et al.*,[4] while ρ_{ss} in the present work is only about half of that obtained by those authors. We can attribute this discrepancy to their failure to account for an electron-electron interaction. Our effective Debye temperature, Θ_D, is about 5% smaller than those obtained from specific-heat measurements (~399 K).[16] This same discrepancy has been found in many metals and has been attributed to the anisotropy of the Fermi surface and the failure to account for the umklapp processes in the electron-phonon interaction.[25-27]

As mentioned earlier, the dominant carriers for thermal conduction in the normal state are electrons. We thus will assume that $K_n=K_{en}$. The parameters obtained for the least-squares fit to

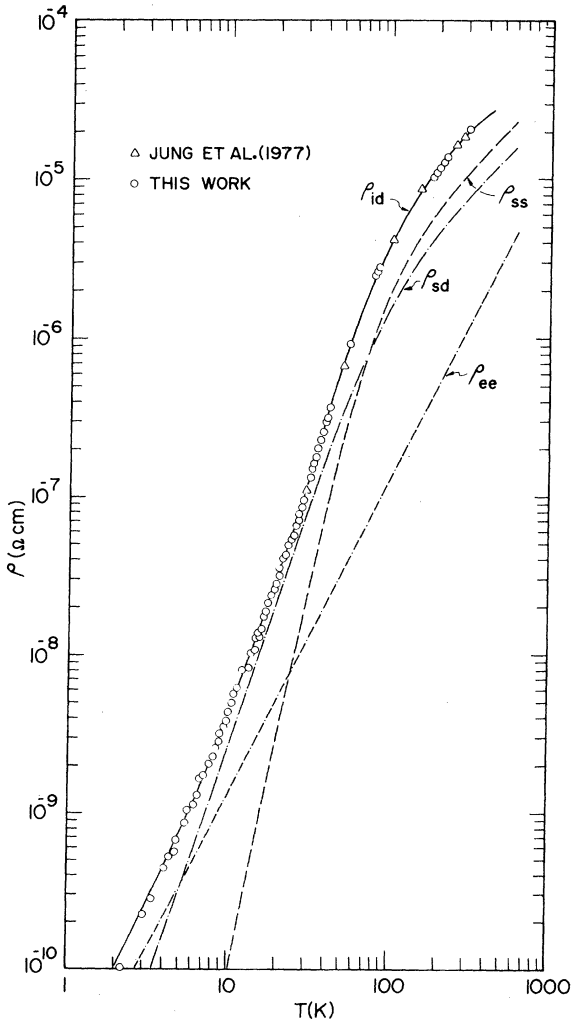

FIG. 4. Experimental data and least-squares fit of $[(T/K)-0.4461]/T^2$ versus T for Sample I.

the measured thermal resistivity also are listed in Table I along with those parameters for electrical resistivity. Figure 5 shows the least-squares fit of $(T/K-\beta_0)/T^2$ or $(\beta_{ee}+\beta_{eb}T)$ vs T for Sample I. If either the electron-electron scattering term or the electron-phonon scattering term is ignored, we find much larger rms deviations than those obtained when both of these scattering terms are included. Additionally, the "residual" thermal resistivity (W_0) obtained by ignoring either the electron-electron scattering or electron-phonon scattering term does not agree with the value calculated using residual electrical resistivity and the Lorenz ratio $L_0=2.45\times10^{-8}$ $(V/K)^2$. By contrast, the agreement was excellent when these scattering terms were included. We note also that our β_{eb}'s for both samples are in good agreement and are consistent with those values obtained by Jung *et al.*[4]

β_{ee} for Sample I is about 1.3×10^{-4} cm/W. However, it is not possible to obtain the β_{ee} term for Sample II because it is less than 2% (as compared to 29% for Sample I) of the residual resistivity at 10 K. Our calculation of ρ_{ee}/β_{ee} for Sample I is 1.0×10^{-8} $(V/K)^2$, which is in agreement with the value obtained from theoretical[28] and other experimental studies.[29]

Our estimate of the residual mean free paths (mfp's) for electrons is 6.2×10^4 Å for Sample I and 2.5×10^3 Å for Sample II. These two mfp's are much longer than the coherence length (ξ_0) for vanadium, which is only about 440 Å.[16] Therefore, our specimens are all in the clean limit for type-II superconductors. It is obvious that the residual mfp's of electrons for these two samples are limited by electron-impurity scattering because both mfp's are three to four orders of magnitude smaller than any of the specimen's dimensions. The dominant contaminants in these two samples were found to be carbon, nitrogen, and oxygen.[14] The average atomic radius for these ions is about 1.4 Å, yielding a classical scattering cross section of $\langle\sigma\rangle=\frac{3}{2}\pi r^2=9.3\times10^{-16}$ cm^2. From elementary kinetic theory, the mfp of an electron is $l=1/N_i\langle\sigma\rangle$, where N_i represents the impurity concentration. Using this expression, we obtained, for Sample I, $N_i=1.7\times10^{18}$ cm^{-3} and $N_i/N=24\times10^{-6}$ or 24 ppm; for Sample II, $N_i=4.3\times10^{19}$ cm^{-3} and $N_i/N=597\times10^{-6}$ or 597 ppm, where N is the number density of atoms. These two resulting concentrations, 24 ppm and 597 ppm, are in reasonable agreement with an extrapolation from the work of Carlson *et al.*[14]

The intrinsic thermal resistivity due to the electron-phonon intraband scattering varies as T^2. However, the electron-phonon interband scattering also produces a thermal resistivity proportional to T^2. Thus, it is impossible to distinguish one contribution from the other solely from an analysis of the thermal resistivity. This difficulty can be resolved by applying the Wiedemann-Franz law in conjunction with electrical resistivity measurements, thus allowing us to estimate the contributions of both s-d and s-s scattering.[30]

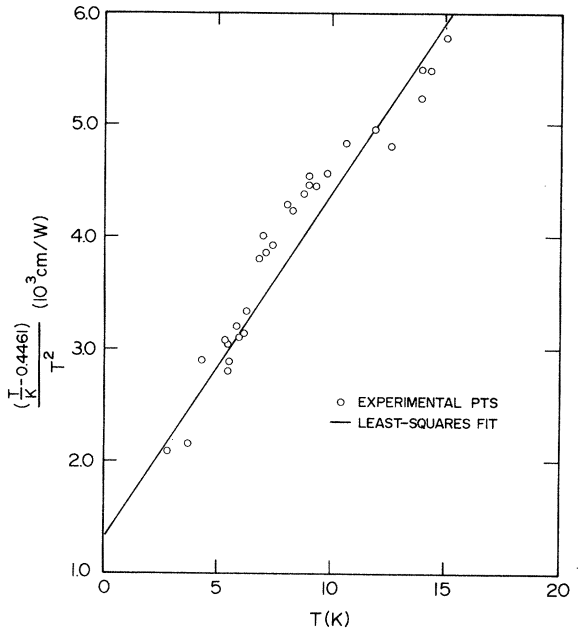

FIG. 5. ρ_{id} versus T for Sample I, showing the contributions due to electron-electron scattering (ρ_{ee}), electron-phonon intraband scattering (ρ_{ss}), and electron-phonon interband scattering (ρ_{sd}). Some ρ_{id} data for $T>10$ K are shown from the work of Jung *et al.* (Ref. 4).

If $\Gamma_{sd}(T)$ is the thermal resistivity as limited only by s-d scattering, then

$$\Gamma_{sd}(T)=\frac{1}{L_0}\rho_{sd}T^2 .$$

Resulting evaluation yields

$$\Gamma_{sd}(T)=1.12\times10^{-4}T^2 \text{ cm K/W for } T\to0$$

or

$$\beta_{sd}=1.12\times10^{-4} \text{ cm/WK}.$$

Combining this evaluation with the Sample I result that

$$\beta_{eb}=\beta_{sd}+\beta_{ss}=3.09\times10^{-4} \text{ cm/WK},$$

we find that

$$\beta_{ss}=1.97\times10^{-4} \text{ cm/WK}.$$

That is, at low temperature and excluding electron-electron scattering, interband scattering contributed about 35% of the total thermal resistivity, while intraband scattering contributed 65%.

In addition, since

$$\Gamma_{sd}(\infty)+\Gamma_{ss}(\infty)=\lim_{T\to\infty}\frac{1}{L_0T}\left(\rho_{sd}T^3\frac{J_3(\Theta_D/T)}{7.212}+\rho_{ss}T\frac{J_3(\Theta_D/T)}{124.43}\right),$$

then we obtain $\Gamma_{ep}(\infty)+\Gamma_{sd}(\infty)=2.75\,(\mathrm{cm\,K})/\mathrm{W}$, in agreement with the value obtained by White and Woods.[23]

One of the major reasons for carrying out transport measurements (as in the current study) is to obtain information about the Fermi surfaces of charge carriers. Ziman calculated the thermal resistivity Γ_{ss} due to s-s scattering and found[24] that

$$\Gamma_{ss}(T)=\beta_{ss}T^2=\frac{12}{\pi^2}J_5(\infty)\left(\frac{k_F}{q_D}\right)^2\frac{\rho_0^{ss}}{L_0\Theta_D^3}T^2. \tag{6}$$

Our best fit to the electrical resistivity data yielded $\Theta_D=380$ K. Subsequently, the electrical resistivity, ρ_Θ^{ss}, due to s-s scattering at $T=\Theta$, is

$$\rho_\Theta^{ss}=14.3\ \mu\Omega\,\mathrm{cm}.$$

Based on the parameters $\beta_{ss}=1.97\times10^{-4}$ cm/WK, $\Theta_D=380$ K, $\rho_0^{ss}=14.3\ \mu\Omega$ cm, and sound velocity, $v_s=3.14\times10^5$ cm/s, we found for the Fermi-surface wave number

$$k_F\simeq 5.2\times10^7\ \mathrm{cm}^{-1}.$$

This value is larger than, but on the same order of magnitude as that (4.2×10^7 cm^{-1}) for a band-structure calculation of the Fermi surface[31] at the N point, which corresponds to a hole band.[31,32] Our value also is in qualitative agreement with the positive sign found experimentally for the thermoelectric power,[4,33] indicating that holes are the dominant charge carriers at low temperatures. The difference between the theoretical k_F and our experimental k_F arises because we have ignored the contributions of the other carriers to the thermal conductivity. Consequently, we determine that the effective-carrier concentration (N_a) is about

$$N_a=\frac{n}{N}=0.45,$$

where n is the carrier concentration and N is the atomic density.

B. Analysis of thermal conductivity in the superconducting state

The superconducting transition temperatures of our samples are 5.43 K and 5.37 K, respectively. Below T_c, the thermal conductivity in the superconducting state (shown in Fig. 2) decreases dramatically with temperature. This decrease of the thermal conductivity in the superconducting state is due primarily to the decrease in the contribution from normal electron transport. Below 1.5 K, the decrease of the thermal conductivity K_s becomes less pronounced. Furthermore, in Sample II, the thermal conductivity K_s shows an increase as temperature decreases around 1.0 K. This behavior is clearly due to the dominant role of the lattice conductivity below 1.5 K and is observed for many elemental superconductors.

We note that electron-impurity scattering is dominant in the electron subsystem below T_c. Thus, the electronic contribution to the thermal conductivity in the superconducting state, K_{es}, can be approximated from BRT (Bardeen, Rickayzen, and Tewordt) theory,[34] or

$$\left(\frac{K_{es}}{K_{en}}\right)^{\mathrm{BRT}}=\frac{1}{F(0)}\left(F(-y)+y\ln(1+e^{-y})+\frac{y^2}{2(1+e^y)}\right), \tag{7}$$

where $y=[\Delta(\tau)/\Delta(0)][\Delta(0)/k_BT_c](1/\tau)$, and $2\Delta(\tau)$ is the BCS expression for the energy gap at the reduced temperature, $\tau=(T/T_c)$. The term $F(-y)$ is given by the expression

$$F(-y)=\int_0^\infty\frac{z\,dz}{(1+e^{y+z})}.$$

Our fit of K_{es}/K_{en} for the Samples I and II as shown in Fig. 6, yields $2\Delta(0)/k_BT_c=3.386$, which is (though smaller) in good agreement with that obtained from specific-heat[17] or tunneling measurements.[35] It is clear from Fig. 6 that the deviation of $(K_{es}/K_{en})^{\mathrm{BRT}}$ from $(K_s/K_n)^{\mathrm{expt}}$ starts at about $\tau\simeq0.27$ (or 1.5 K). Below this temperature, the lattice conductivity becomes more important, particularly for the case of Sample II, the less-pure sample.

The lattice conductivity in the superconducting state, K_{gs}, is determined from the relation

$$K_{gs}=K_s-K_n\left(\frac{K_{es}}{K_{en}}\right)^{\mathrm{BRT}}. \tag{8}$$

The resulting values for K_{gs} are shown in Fig. 7.

The lattice conductivity is generally fit by[36]

$$K_{gs}=\frac{k_B}{2\pi^2v_S}\left(\frac{k_BT}{\hbar}\right)^3\times\int_0^{\Theta_D/T}\frac{x^4e^x\,dx}{(e^x-1)^2[B+CxTg(x,T)+Mx^4T^4]}, \tag{9}$$

where B is related to phonon-boundary scattering, CxT to phonon-electron scattering, while Mx^4T^4 is due to phonon-impurity scattering, with $x=\hbar v_sq/k_BT$. The factor $g(x,T)$ is proportional to the number of normal electrons available (when the sample is superconducting) to scatter phonons.[34]

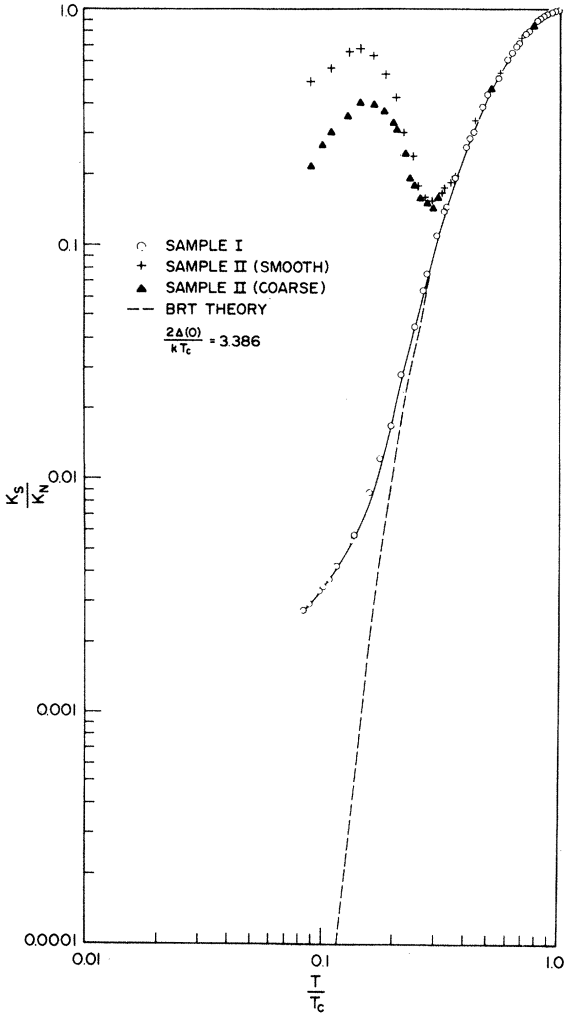

FIG. 6. K_s/K_n versus reduced temperature (T/T_c) for Samples I and II, showing comparison with BRT theory. Data for both surface conditions of Sample II are shown.

The phonon-boundary scattering found for both samples is close to that predicted theoretically. The increase in boundary scattering for Sample II due to sanding (of its surfaces) can be understood easily in terms of decreased specular reflection for phonons. We should note here that the decrease in thermal conductivity due to surface sanding seems to rule out the possible contribution of normal electrons near a second energy gap which had been proposed for transition metals.[37]

These lattice thermal-conductivity results provide valuable information on the electron-phonon interaction. Curve fitting (see Fig. 7) gives the electron-phonon interaction constant C which appears in Eq. (9) and is found to be $(3.1 \pm 0.1) \times 10^9$ $K^{-1}s^{-1}$. This value of C can be obtained also from

TABLE II. Parameters for lattice thermal conductivity.

Sample	B (s^{-1})	M ($K^{-4}s^{-1}$)	C ($K^{-1}s^{-1}$)
I	4.8×10^6	~10	3.3×10^9
II	7.2×10^5	~200	3.1×10^9
II[a]	1.6×10^6	~200	3.1×10^9

[a] Sample II after sandblasting.

the approximation.[38]

$$(K^e_{gs}/K^e_{gn}) = 0.96 \exp[\Delta(0)/k_B T] \text{ as } T \ll T_c , \quad (10)$$

where K^e_{gs} and K^e_{gn} are the lattice conductivities as limited only by electron scattering in the superconducting and normal states, respectively. For a vanadium specimen and in the normal state,

$$K^e_{gn} = 3.6 \times 10^4 T^2/C \quad (11)$$

given in units of W/(K cm).

The lattice conductivity in the superconducting state K^e_{gs} is calculated from

$$K^e_{gs} = (K^{-1}_{gs} - K^{-1}_{gd})^{-1} , \quad (12)$$

where K_{gd} is the lattice conductivity as limited by boundary and defect scattering, and was obtained by a T^3-law extrapolation to higher temperatures. The results for K^e_{gs} are shown in Fig. 8. The best fit for K^e_{gs} was found to be

$$K^e_{gs} = 1.12 \times 10^{-5} T^2 \exp(1.693\tau) , \quad (13)$$

again in units of W/K cm. The deviation of this fit at the lower temperatures in Fig. 8 may be due to the dominant role of boundary scattering. However, combining Eqs. (10), (11), and (12) with the value obtained above for K^e_{gn}, yields $C = 3.1 \times 10^9$ $K^{-1}s^{-1}$. Putting this result into Eq. (11) gives $K^e_{gn} = 1.2 \times 10^{-5} T^2$, which is negligible compared to K_n, in agreement with our earlier analysis.

We note that the electron-phonon interaction term contains a contribution from both electron-phonon intraband and interband scattering. Roughly estimating[24] for C_{ss}, the electron-phonon interaction constant due to intraband scattering, we find $C_{ss} \lesssim 4.6 \times 10^8$ $K^{-1}s^{-1}$. This value for C_{ss} is certainly smaller than 3.1×10^9 $K^{-1}s^{-1}$. Thus, we attribute this difference to the s-d (or interband) scattering, which is about 3×10^9 $K^{-1}s^{-1}$ according to a calculation by Klemens.[39]

The mass-enhancement factor λ due to the electron-phonon interaction is relatively large for transition metals.[38] This parameter can be obtained from the expression[40]

$$\lambda = E^2_{\text{def}} N(0)/\rho_m v_s^2 , \quad (14)$$

where $N(0)$ is the bare density of states for elec-

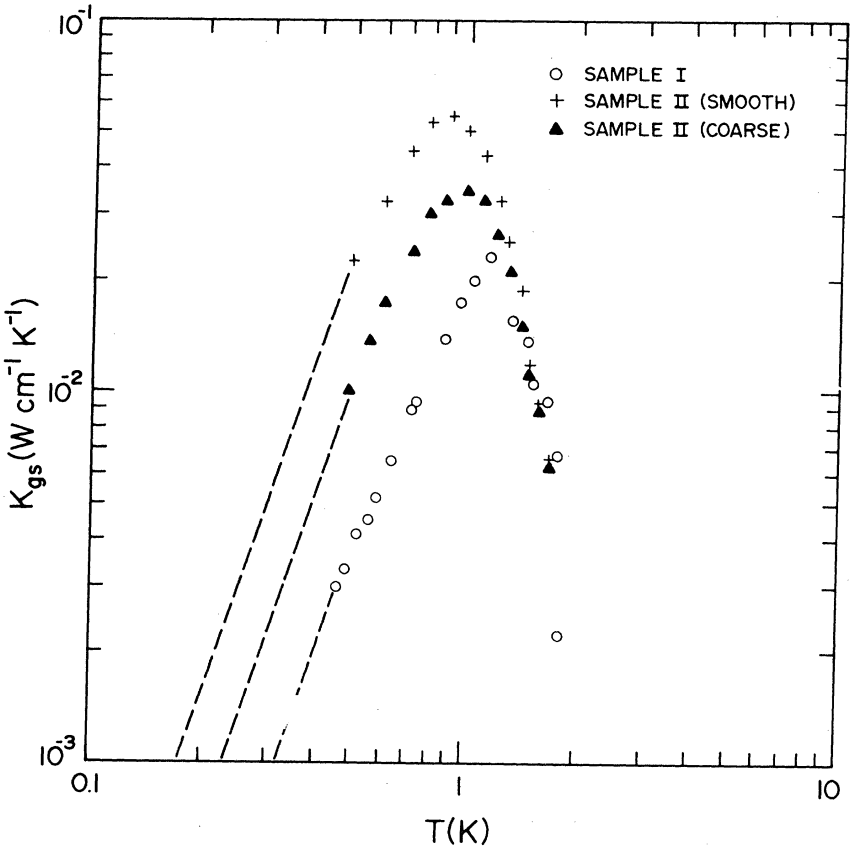

FIG. 7. Calculated superconducting-state-lattice thermal conductivities versus temperature for Samples I and II, based upon Eq. (8). The dotted lines represent extrapolations for lattice conductivity limited only by boundary scattering.

trons and ρ_m is the mass density. The deformation potential, $E_{\rm def}$, can be related to the electron-phonon interaction term C by the following equation[24]:

$$C = \sum_i (m_i^*)^2 \frac{E_{\rm def}^2}{2\pi\rho_m v_s \hbar} \left(\frac{k_B}{\hbar}\right)^3 . \qquad (15)$$

Summation is over the Fermi pockets. Combining our experimental result for C and specific-heat measurement[17] as well as band-structure data,[31,32] yields $\lambda = 0.69$, in agreement with the value obtained from specific-heat[17] and tunneling-effect measurements.[35]

IV. CONCLUSIONS

Consistency in the above analysis for both the electrical and thermal conductivities of high-purity vanadium samples has led us to the conclusion that electron-phonon interband scattering (or s-d scattering) is the dominant factor in determining the values of both thermal and electrical resistivity above 100 K and of the thermal resistivity in the low-temperature range reported here.

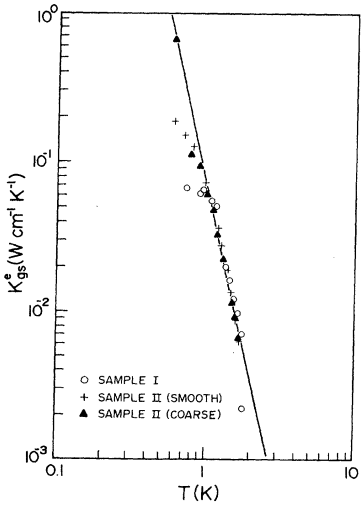

FIG. 8. Calculated superconducting-state-lattice thermal conductivities versus temperature for Samples I and II, assuming scattering only by electrons, based upon Eq. (12). The solid line represents a best fit.

Although electron-electron scattering appears unimportant for both thermal and electrical resistivities at higher temperatures, this scattering mechanism is significant in determining both transport properties in the liquid-helium temperature range.

The thermal conductivity in the superconducting state was found to be in agreement with BRT theory, indicating that electron-impurity scattering is still dominant below T_c. The lattice conductivity deduced from the thermal conductivity in the superconducting state yielded information of phonon-boundary scattering, as well as of the phonon-electron interaction. The mass-enhancement factor λ calculated from the deformation potentials of electrons, is in agreement with that obtained from specific-heat and tunneling measurements.

ACKNOWLEDGMENTS

We are grateful to Dr. C. W. Thompson, Jr. for his help and advice, and to Professor C. K. Chau for his early interest in this study. This work was supported by the U. S. Department of Energy.

---

*Present address: Institute of Chemical Analysis, Northeastern University, Boston, MA 02115.
†Present address: S. H. E. Corporation, 4174 Sorrento Blvd., San Diego, CA 92121.

[1]D. K. Wagner, Phys. Rev. B 5, 336 (1972).
[2]H. Weinstock, C. L. Tsai, and F. A. Schmidt, J. Phys. (Paris) C-6, 1024 (1978).
[3]H. M. Rosenberg, Trans. R. Soc. London A 247, 441 (1955); G. K. White and S. B. Woods, Can. J. Phys. 35, 892 (1957); J. P. Burger and M. A. Taylor, Phys. Rev. Lett. 6, 185 (1961); W. Rastaker and A. S. Yamamoto, Trans. Am. Soc. Met. 47, 1002 (1955); Y. M. Smirnov and V. A. Finkel, Zh. Eksp. Teor. Fiz. 49, 1077 (1965) [Sov. Phys.—JETP 22, 756 (1966)]; G. K. White and S. B. Woods, Philos. Trans. R. Soc. A 251, 273 (1959); H. Suzuki, S. Minomura, and S. Miyahara, J. Phys. Soc. Jpn. 21, 2089 (1966); B. K. Chakalskii, N. A. Redko, S. S. Shalyt, and V. M. Ashazha, Zh. Eksp. Teor. Fiz. 75, 1320 (1978) [Sov. Phys.—JETP 48, 665 (1978)].
[4]W. D. Jung, F. A. Schmidt, and G. D. Danielsen, Phys. Rev. B 15, 659 (1977).
[5]R. A. Guenther, Ph.D. thesis, Illinois Institute of Technology, 1969 (unpublished); R. A. Guenther and H. Weinstock, J. Appl. Phys. 42, 3790 (1971).
[6]C. L. Tsai, Ph.D. thesis, Louisiana State University, 1976 (unpublished).
[7]G. K. White, *Experimental Techniques in Low Temperature Physics* (Oxford University Press, London, 1968).
[8]C. W. Thompson, Jr., Ph.D. thesis, Illinois Institute of Technology, 1978 (unpublished).
[9]Scientific Instruments Inc., 632 S. F. Street, Lake Worth, FL 33460.
[10]Lake Shore Cryotronics, Inc., 64 E. Walnut Street, Westerville, OH 43081.
[11]P. H. Kes, A. M. van der Klein, and D. de Klerk, Cryogenics 14, 168 (1974).
[12]S. H. E. Manufacturing Corp., 4174 Sorrento Valley Blvd., San Diego, CA 92121.
[13]G. W. Webb, Phys. Rev. 181, 1127 (1969).
[14]O. N. Carlson, F. A. Schmidt, and D. G. Alexander, Met. Trans. 3, 1249 (1972).
[15]R. L. Fagaly, F. A. Schmidt, and H. Weinstock, Cryogenics 19, 58 (1979).
[16]S. T. Sekula and R. H. Kernohan, Phys. Rev. B 5, 904 (1972).
[17]H. A. Leupold, G. J. Iafrate, F. Rothwarf, J. T. Breslin, D. Edminston, and T. R. Aucoin, J. Low Temp. Phys. 28, 241 (1977); R. Radebaugh and P. H. Keesom, Phys. Rev. 149, 217 (1966).
[18]N. F. Mott, Proc. R. Soc. London 47, 571 (1935).
[19]J. Appel, Philos. Mag. 8, 1971 (1963).
[20]T. L. Ruthruff, C. G. Grenier, and R. G. Goodrich, Phys. Rev. B 17, 3070 (1978); also, the papers cited in this article.
[21]N. F. Mott and H. H. Wills, Proc. R. Soc. London A153, 699 (1936).
[22]A. H. Wilson, Proc. R. Soc. London A 167, 580 (1938).
[23]G. K. White and S. B. Woods, Philos. Trans. R. Soc. London A 251, 273 (1959).
[24]A. H. Wilson, *The Theory of Metals* (Cambridge University Press, London, 1958); J. M. Ziman, *Electrons and Phonons* (Oxford University Press, London, 1960).
[25]J. Bass, Adv. Phys. 21, 431 (1972).
[26]J. M. Ziman, *Electrons and Phonons* (Oxford University Press, London, 1960); F. J. Blatt, *Physics of Electronic Conduction in Solids* (McGraw-Hill, New York, 1968).
[27]J. W. Ekin, Phys. Rev. B 6, 371 (1972); M. J. Laubitz and J. G. Cook, Phys. Rev. B 6, 2082 (1972).
[28]C. Herring, Phys. Rev. Lett. 19, 167 (1967).
[29]G. K. White and R. J. Tanish, Phys. Rev. Lett. 19, 165 (1967).
[30]J. G. Cook, M. P. Van der Meer, and M. J. Laubitz, Can. J. Phys. 50, 1386 (1972).
[31]L. F. Mattheiss, Phys. Rev. B 1, 373 (1970); M. Yasui, E. Hayashi, and M. Shimizu, J. Phys. Soc. Jpn. 29, 1446 (1970); D. Papaconstantopoulos, J. R. Anderson, and J. W. McCaffrey, Phys. Rev. B 5, 1214 (1971); S. Wakoh and J. Yamashita, J. Phys. Soc. Jpn. 35, 1394 (1973); L. L. Boyer, D. Papaconstantopoulos, and B. M. Klein, Phys. Rev. B 15, 3685 (1977); D. G. Laurent, J. Callaway, and C. S. Wang, Phys. Rev. B 20, 1134 (1979).
[32]R. D. Parker and M. H. Halloran, Phys. Rev. B 9, 4130 (1974).
[33]A. R. Mackintosh and L. Sill, J. Phys. Chem. Solids 24, 501 (1963).
[34]J. Bardeen, G. Rickayzen, and L. Tewordt, Phys. Rev. 113, 982 (1959).

[35]P. G. deGennes, *Superconductivity of Metals and Alloys* (Benjamin, New York, 1966).
[36]Based on the Debye model and ignoring the three-phonon normal processes. J. Callaway [Phys. Rev. 113, 1046 (1959)] had calculated the thermal conductivity with a correction term for three-phonon normal processes, which we regard as a negligible term in this study.
[37]R. Radebaugh and P. H. Keesom, Phys. Rev. 149, 217 (1966).
[38]A. C. Anderson and S. G. O'Hara, J. Low Temp. Phys. 15, 323 (1974).
[39]P. G. Klemens, in *Solid State Physics*, edited by F. Seitz and D. Turnbull (Academic, New York, 1958), Vol. 7.
[40]J. Callaway, *Quantum Theory of the Solid State* (Academic, New York, 1973).